JOURNAL OF AGRICULTURAL AND FOOD CHEMISTRY

Subscriber access provided by READING UNIV

Article

Discovery of New 2-[(4,6-Dimethoxy-1,3,5-triazin-2-yl)oxy]-6-(substituted phenoxy)benzoic Acids as Flexible Inhibitors of Arabidopsis thaliana Acetohydroxyacid Synthase and Its P197L Mutant

Ren-Yu Qu, Jing-Fang Yang, DEVENDAR PONNAM, Wei-Ming Kang, Yu-Chao Liu, Qiong Chen, Cong-Wei Niu, Zhen Xi, and Guang-Fu Yang

J. Agric. Food Chem., **Just Accepted Manuscript** • DOI: 10.1021/acs.jafc.7b05198 • Publication Date (Web): 30 Nov 2017

Downloaded from http://pubs.acs.org on December 1, 2017

Just Accepted

"Just Accepted" manuscripts have been peer-reviewed and accepted for publication. They are posted online prior to technical editing, formatting for publication and author proofing. The American Chemical Society provides "Just Accepted" as a free service to the research community to expedite the dissemination of scientific material as soon as possible after acceptance. "Just Accepted" manuscripts appear in full in PDF format accompanied by an HTML abstract. "Just Accepted" manuscripts have been fully peer reviewed, but should not be considered the official version of record. They are accessible to all readers and citable by the Digital Object Identifier (DOI®). "Just Accepted" is an optional service offered to authors. Therefore, the "Just Accepted" Web site may not include all articles that will be published in the journal. After a manuscript is technically edited and formatted, it will be removed from the "Just Accepted" Web site and published as an ASAP article. Note that technical editing may introduce minor changes to the manuscript text and/or graphics which could affect content, and all legal disclaimers and ethical guidelines that apply to the journal pertain. ACS cannot be held responsible for errors or consequences arising from the use of information contained in these "Just Accepted" manuscripts.

ACS Publications

Journal of Agricultural and Food Chemistry is published by the American Chemical Society. 1155 Sixteenth Street N.W., Washington, DC 20036

Published by American Chemical Society. Copyright © American Chemical Society. However, no copyright claim is made to original U.S. Government works, or works produced by employees of any Commonwealth realm Crown government in the course of their duties.

Discovery of New 2-[(4,6-Dimethoxy-1,3,5-triazin-2-yl)oxy]-6-(substituted phenoxy)benzoic Acids as Flexible Inhibitors of *Arabidopsis thaliana* Acetohydroxyacid Synthase and Its P197L Mutant

Ren-Yu Qu,[†] Jing-Fang Yang,[†] Ponnam Devendar,[†] Wei-Ming Kang,[†] Yu-Chao Liu,[†] Qiong Chen,[†] Cong-Wei Niu, [‡] Zhen Xi, [*,‡,#] and Guang-Fu Yang[*,†,#]

[†]*Key Laboratory of Pesticide & Chemical Biology of Ministry of Education, College of Chemistry, Central China Normal University(CCNU), Wuhan 430079, P. R. China*

[‡]*State Key Laboratory of Elemento-Organic Chemistry, Nankai University (NKU), Tianjin 300071, P. R. China*

[#]*Collaborative Innovation Center of Chemical Science and Engineering, Tianjin 30071, P.R. China.*

AUTHOR INFORMATION

***Corresponding Authors:**

Tel: +86-27-67867800, Fax: +86-27-67867141, E-mail: gfyang@mail.ccnu.edu.cn.

Tel: +86 022-23504782, Fax: +86 022-23504782, E-mail: zhenxi@nankai.edu.cn.

ORCID:

Guang-Fu Yang: 0000-0003-4384-2593

Zhen Xi: 0000-0002-3332-5413

ABSTRACT: In the search for new anti-resistance acetohydroxyacid synthase (AHAS, EC 2.2.1.6) inhibitors to combat weed resistance associated with AHAS mutations, a series of 2-[(4,6-dimethoxy-1,3,5-triazin-2-yl)oxy]-6-(substituted phenoxy)benzoic acids **11**–**38** were designed and synthesized via the strategy of conformational flexibility analysis. Compounds **21**, **22**, **26**, **33**, **36** and **38** with high potency against both wild-type *At*AHAS and its P197L mutant were identified as promising candidates with low resistance factors (*RF*, defined as the ratio between the k_i values towards P197L mutant and wild type AHAS) ranging from 0.73 to 6.32. Especially, compound **22** (*RF* = 0.73) was further identified as the most potent anti-resistance AHAS inhibitor due to its significantly reduced resistance level compared with tribenuron-methyl (*RF* = 2650) and bispyribac (*RF* = 4.57). Furthermore, compounds **26**, **33**, **36** and **38** also displayed promising herbicidal activities against sensitive and resistant (P197L) *Descurainia sophia* at the dosage of 75–150 g of active ingredient (ai)/ha. Notably, compounds **33** and **38** still maintained over 60% herbicidal activity toward the resistant weed even at much lower dosages (37.5 g.ai/ha). Therefore, the designed scaffold has the great potential to discover new candidate compounds for the control of weed resistance associated with AHAS mutation.

KEYWORDS: AHAS inhibitors, structure-activity relationship, anti-resistance property, P197L mutant, herbicidal activity, molecular docking

INTRODUCTION

Acetohydroxyacid synthase (AHAS, EC 2.2.1.6), an essential enzyme in the branched-chain amino acids (BCAAs) biosynthesis, mainly catalyzes the synthesis of 2-aceto-2-hydroxybutyrate and 2-acetolactate via condensation of a single molecule of 2-ketobutyrate with a single molecule of pyruvate (the pathway of isoleucine biosynthesis) or two molecules of pyruvate (the pathways of leucine and valine biosynthesis), respectively. It has been considered to be an attractive target for both drug and agrochemical discovery due to its special biological functions and gene conservation throughout diverse species (plants, bacteria, fungus, algae).[1-3] In particular, AHAS has a great importance in the field of herbicide research, and it is a target of five classes of herbicides, including triazolopyrimidine sulfonamides (TPs), sulfonylureas (SUs), pyrimidinyl-(thio)benzoates (PTBs), sulfonylamino-carbonyl-triazolinones (SCTs) and imidazolinones (IMIs) (Figure 1).[4-7]

Unfortunately, AHAS-inhibiting herbicides are facing serious weed resistance due to their long-term overuse in agricultural applications and possession of only a single ligand-binding site in AHAS.[8-10] Weed resistance to AHAS inhibitors is mainly caused by single-point mutations in the region of the binding site, causing a reduction in the binding affinity between the AHAS and its inhibitors.[9-12] According to a recent survey, the biotypes of 144 weed species have evolved different degrees of resistance to AHAS herbicides globally, and this number is increasing year after year.[13-15] In all the surveyed 144 resistant weed species associated with AHAS mutations, the mutation at Pro-197 is the most common cause of resistance to AHAS inhibitors (there are about 70 resistant weeds caused by mutation at Pro-197),[16, 17] and 8 types of mutations (Ala, Thr, Ser, Arg, Gln, Leu, His, Ile substitutions) are involved in Pro-197.[8, 18-21]

There are currently several commercialized AHAS herbicides which show similar inhibitory activities against wild-type AHAS as well as its P197 mutants,[22] for example, imazaquin, imazapyr, pyrithiobac and bispyribac have low degrees of resistance against Pro-197-Ser or Pro-197-His mutants. More importantly, weed resistance caused by the Pro-197-Leu mutation has been extensively reported around the world, and this mutant has caused serious cross-resistance to most types of AHAS inhibitors. For example, the resistance levels for most sulfonylureas and other AHAS herbicides (in IMIs, TPs and PTBs) have been increased up to more than 100-fold and 10-fold respectively, as a result of Pro-197-Leu mutation.[23-27] However, reports of novel anti-resistance herbicides active against Pro-197-Leu mutation in AHAS are quite rare. Therefore, the development of a new anti-resistance AHAS inhibitor with a strong *in vitro* and *in vivo* activity against P197L mutant is highly desirable. In the current study, we have sought to design and synthesize novel AHAS inhibitors with such activities.

There are several solutions to combat mutation-linked drug resistance. For example, drug combinations, multiple targeting design, targeting highly conserved residues, targeting protein backbone and conformational flexibility drug design. In our previous work, we discovered that the ligand conformation of sulfonylurea and triazolopyrimidine sulfamide AHAS inhibitors did not undergo any significant changes in wild-type *At*AHAS and its mutants because of their rigid bridges ($SO_2NHCONH$ and SO_2NH). As a result, these inhibitors no longer interact with the key amino acids or they cause steric hindrance with mutants, and that is the resistance mechanism for these inhibitors.[28-31] Therefore, developing AHAS inhibitor with conformational flexibility should be an effective method to overcome resistance caused by mutation. On the basis of this strategy, we have recently reported the syntheses, *At*AHAS inhibitory and anti-resistance

activities of 2-aroxyl-1,2,4-triazolopyrimidines,[32, 33] and 2-benzoyloxy-6-pyrimidinyl salicylic acids,[34] which have flexible ether bridges. In particular, diaryl ether has received a great deal of attention in the area of agrochemistry.[35, 36] For instance, cyhalofop-butyl (ACCase inhibitor) and fomesafen (PPO inhibitor) have been used as popular commercial herbicides to eradicate weeds in the past decade. Additionally, the other commercial fungicides containing diaryl ether, such as quinoxyfen, famoxadone, tolfenpyrad and metominostrobin, could effectively control plant pathogens.[37, 38]

In our continuing endeavor to seek new anti-resistance AHAS inhibitors, we design a scaffold by inserting a flexible ether linker in between triazinyl and phenyl ring of sulfonylureas (Figure 2). Some commercial examples of sulfonylureas include chlorsulfuron, metsulfuron-methyl, tribenuron-methyl, chlorimuron-ethyl and iodosulfuron-methyl, which are not effective against weeds with the Pro-197-Leu mutation in AHAS.[39, 40] Also, the binding model shows that the designed scaffold having an *ortho*- carboxylic acid group potentially can accommodate additional hydrogen bonding interactions with the binding site (R377, K256, etc.). Further, we introduced phenoxy groups on the designed scaffold (*meta*-position) to increase the conformational flexibility, and these final structures may lead to the discovery of anti-resistance AHAS inhibitors (Figure 2). Herein, we synthesized the designed compounds **11**–**38**, measured the inhibitory effects (against both wild-type *At*AHAS and P197L mutant), anti-resistance properties, and herbicidal activities (against sensitive and resistant *Descurainia sophia*). We proposed the binding models of the designed compounds and performed molecular docking, dynamics simulations and Molecular Mechanics Poisson-Boltzmann Surface Area (MM-PBSA) calculations.

MATERIALS AND METHODS

Chemicals and Instruments. All purchased reagents were used as receives, if not specified otherwise. Organic solvents were also directly used without further purification, such as dimethylformamide (DMF), acetic acid (AcOH), and methanol (MeOH). Using tetramethylsilane (TMS) as the internal reference, ^{1}H NMR and ^{13}C NMR spectra were recorded in $CDCl_3$ or DMSO-d_6 as solvent on a Mercury-Plus 400 or 600 MHz spectrometer (Varian, Palo Alto, CA). A model B-545 melting point apparatus (Büchi, Flawil, Switzerland) was used to obtain melting points without calibration. High-resolution mass spectra (HRMS) data was determined with 6224 TOF LC/MS (Agilent Technologies, Santa Clara, CA) instrument. The column used was a 250 mm × 4.6 mm i.d., 5 μm, Eclipse XDB-C18 (Agilent Technologies, Santa Clara, CA). The flow rate, injection volume and column temperature were set to 0.2 mL/min, 2.0 μL and 25 °C, respectively. Mass spectrometry (MS) was conducted on a DSQII GC-MS (Thermo Fisher, Austin, TX) instrument with an electrospray ionization (ESI) source. The heat temperature was from 50 to 300 °C (heating rate of 20 °C /min) and scan ranges of m/z 100–500 for MS. The GC column used was a 30 m × 0.25 mm i.d., 0.25 μm (film thickness), Zebron ZB-35 HT Inferno (Phenomenex, Torrance, CA).

Synthetic Chemistry. The synthesis of the target compounds **11**–**38** is illustrated in Figure 3. The synthesis included seven steps from the commercially available 3-flouroanisole, compound **1**, as the starting material. The regioselective formylation of **1** with N,N-Dimethylformamide (DMF) using *n*-BuLi/TMEDA/DIPA (*in situ* deprotonation/metalation) afforded the aldehyde **2**. The aldehyde **2** when treated with diverse substituted phenols **3aa**–**bb** using K_2CO_3 in DMF gave 2-methoxy-6-(substituted

phenoxy)benzaldehydes **4aa**–**bb**. The subsequent oxidation of the formyl group of the molecules **4aa**–**bb** were achieved by using 30% H_2O_2 and 50% aq. KOH in MeOH followed by acidification, which resulted 2-methoxy-6-substitutedphenoxybenzoic acids **5aa**–**bb**. The acids **5aa**–**bb** were subjected to the demethylation reaction by treating with BBr_3 which yielded hydroxy acids **6aa**–**bb**. In the next step, the acid groups of **6aa**–**bb** were protected with benzyl bromide **7** using $KHCO_3$ in DMF leading to the corresponding benzyl esters **8aa**–**bb**. The crude compounds **8aa**–**bb** were then treated with 2-chloro-4,6-dimethoxy-1,3,5-triazine **9** using K_2CO_3 in DMF, yielding compounds **10aa**–**bb**. In the final step, the ester hydrolysis of crude compounds **10aa**–**bb** with H_2 and Pd/C in CH_3OH/AcOH generated the desired target compounds **11**–**38**. The chemical structures of the synthesized target compounds were established by ^{1}H NMR, ^{13}C NMR and HRMS data. Further, the single crystal structure of compound **22** was confirmed by X-ray diffraction (Figure 4).

X-ray Diffraction. Compound **22** was crystallized from a mixture of *n*-hexane and chloroform to give colorless crystals suitable for single crystal X-ray analysis. Crystals **22** (0.20 mm × 0.15 mm × 0.15 mm) were mounted in fluoropolyether oil. On a Bruker SMART APEX DUO CCD area detector diffractometer (Bruker AXS, Madison, WI), cell dimensions and intensities were measured at 296 K with graphite-monochromated Mo Kα radiation λ = 0.71073 Å; θ_{max} =26.00; 15699 measured reflections; 4131 independent reflections R_{int}= 0.0231. Data integration and data reduction were carried out with the SAINT Plus program. The intensity data were corrected for Lorentz, polarization and absorption effects (T_{max} = 0.9848; T_{min} =0.9799). The structure was solved by direct method using SHELXS97 and refined with

151 SHELXL970. Based on F^2 using the weight of $1/[\sigma^2(F_0^2) + (0.0788P)^2 + 0.3909P]$, full-matrix
152 least-squares refinement gave final values of $R_1 = 0.0388$, $\omega R_2 = 0.1157$, and GOF(F) = 1.044
153 for 303 variables, 303 parameters, and 4131 contributing reflections. Maximum/minimum
154 residual electron density = 0.177 per -0.213 e.Å^{-3}, and maximum shift/error = 0.000. Hydrogens
155 were either found or placed in calculated positions and isotropically refined using a riding
156 model. The non-hydrogen atoms were refined anisotropically. We deposited the
157 crystallographic data for compound **22** with the Cambridge Crystallographic Data Centre
158 (CCDC) with deposition no. 1558575.[41]

159 ***At*AHAS Inhibitory Experiments.** As described in our previous studies,[33, 34] the
160 wild-type *At*AHAS and P197L mutant were expressed from the plasmids pET28a
161 (+)-*At*AHAS and pET28a (+)-*At*AHAS-Pro197Leu, respectively. In addition, the *in vitro*
162 inhibitory activity (K_i value) of the synthesized compounds against wild-type *At*AHAS and
163 P197L mutant were studied using the method described previously.[42-44] The results are
164 summarized in Table 1.

165 **Computational Modeling and Calculation of Binding Free Energies.** The crystal
166 structure of wild-type *At*AHAS (PDB ID:5K2O) was taken from the Protein Data Bank.[7] The
167 P197L mutant was introduced to the wild-type ligand-protein complexes by using the
168 biopolymer mutation modeling tool in SYBYL v2.0. The conformations of the mutant
169 complexes were further minimized by using the Powell method of 3000 steps for residues in
170 3Å around the mutational site. The AutoDock v4.2 software was used to dock representative
171 inhibitors into *At*AHAS which clustered by 2 Å of Root-Mean-Square Deviation (RMSD).
172 Criteria and molecule modeling was visualized by PyMOL v1.3. On the basis of the result of

previous 1~2 ns equilibrating Molecular Dynamics (MD) simulation of commercial compounds and the reported crystal structure of bispyribac, we chose the final conformations of target compounds to calculate binding free energy via Molecular-Mechanics Poisson-Boltzmann Surface Area (MM-PBSA) method.[45]

Herbicidal Activity. Sensitive and resistant (Pro-197-Leu in AHAS) *Descurainia sophia* (*D. sophia*) were selected as representative weeds for screening the compounds, and the herbicidal activities were evaluated as described previously.[33, 34] Before testing, all of the synthesized compounds were dissolved in DMF and diluted with Tween-80 (100 mg/mL). The solutions were further diluted with water to the tested concentrations. In the greenhouse, the seeds of *D. sophia* were incubated with 0.05% GA3 solution for 1 day, and then prepared seeds were planted at flowerpots (inner diameter of 7.5 cm) and its growth at temperatures kept at 15 °C (night) and 25 °C (day). When *D. sophia* had grown to the four-leaf stage, they were treated by the inhibitor-containing solutions at the required concentrations (150, 75 or 37.5 g ai/ha). Herbicidal activity was evaluated visually after 35 days via post-emergence treatment, with three replicates per treatment. The results of herbicidal activity of all the compounds are described in Table 2.

RESULTS AND DISCUSSION

Enzyme Inhibition Activities (against P197L Mutant and Wild-Type *At*AHAS) and Structure-Activity Relationship. According to the previously mentioned methods, the inhibition constants (K_i values) of compounds **11**–**38** were investigated against wild-type *At*AHAS and P197L mutant. The commercial AHAS herbicide tribenuron-methyl and

bispyribac were chosen as the positive controls.

Among the 28 newly synthesized compounds (Table 1), most of them exhibited moderate to excellent activities against P197L mutant. In particular, compounds **21** (3,4-benzo**)** and **22** (4-ph) were identified as the most potent inhibitors against P197L mutant with K_i values of 3.17 μM and 2.71 μM respectively. In order to optimize compound **11** (R^1 = H), we initially focused on introducing a single substituent (R^1) on the phenoxy ring, which could affect the enzyme inhibitory activity. In most cases, the different mono substitutions at the *para*- or *meta*- position of the phenoxy ring gave rise to compounds with higher inhibitory activities compared with the compounds modified at the *ortho*- position. Taking the fluorine substituent as an example, the activity of compound **14** (2-F) was reduced to 108.00 μM ($K_{i,\ P197L}$ value), when compared with compounds **16** (4-F, $K_{i,\ P197L}$ = 21.40 μM) and **15** (3-F, $K_{i,\ P197L}$= 60.50 μM). (The same phenomenon applies to chlorine substituent). Additionally compared with the single substituted derivatives **12**–**20** (F, Cl, Me substitution), **31** with 2,4-di-Cl ($K_{i,\ P197L}$= 7.58 μM**)** substitutions at the R^1 position showed increased inhibitory activity against P197L mutant, which implied introducing dual substituted groups on the phenoxy group might enhance the inhibitory activity. Unfortunately, when –Cl at different positions or other halogens (such as –F, -Br) substituents were introduced, the inhibitory activity did not improved and, even in some cases decreased, for instance compounds **23** (2,3-di-F, $K_{i,\ P197L}$= 228.00 μM), **24** (2,4- di-F, $K_{i,\ P197L}$= 84.30 μM), **30** (2,3-di-Cl, $K_{i,\ P197L}$= 75.70 μM), **32** (2,5-di-Cl, $K_{i,\ P197L}$= 55.30 μM) and **37** (3-Br-4-F, $K_{i,\ P197L}$= 145.00 μM). However, upon introducing both a methyl group and a halogen atom on the phenoxy ring, the inhibitory activity improved as compared with the compounds with a single substitution (**12**–**20**). For example, the inhibitory activities of compounds **26** (2-F-3-CH_3, $K_{i,}$

$_{P197L}$= 3.35 μM), **33** (2-Cl-4-CH_3, $K_{i, P197L}$= 3.70 μM), and **38** (3-CH_3-4-Br, $K_{i, P197L}$= 3.34 μM) reached a micromolar level, which were more than 55-fold higher than the commercial control tribenuron-methyl ($K_{i, P197L}$=212.00 μM).

At the same time, larger sterically hindered structures also had a favorable effect on increasing the inhibitory activity. For example, compounds **21** (3,4-benzo, $K_{i, P197L}$= 3.17 μM) and **22** (4-Ph, $K_{i, P197L}$= 2.71 μM) showed higher activity than **11** ($K_{i, P197L}$= 52.80 μM) and almost similar activity to bispyribac ($K_{i, P197L}$= 2.47 μM). We then pursued the experiments with molecular modeling to analyze the binding mode of the representative compound **21** with the P197L mutant. As shown in Figure 5A, compound **21** had a conservative π-π stacking interaction with W574 and its carboxyl group formed strong hydrogen bonds with many residues in the P197L mutant AHAS, such as G120, K256, R377 and S653. Although all the compounds had similar binding pattern with compound **21,** the van der Waals (VDW) interactions and binding free energy were all remarkably enhanced in presence of steric hindrance on the structures (compounds **21** and **22**) (Table S1). We conclude that, hybrids of triazine-salicylic acids (phenoxy-substituted) connecting through ether bridges could therefore be used as a new scaffold for discovering novel AHAS inhibitors against P197L mutant.

Interestingly, most of the compounds exhibited good enzyme inhibiting activities against wild-type *At*AHAS as well. As shown in Table 1, compound **11** (R^1= H) exhibited good activity ($K_{i, WT}$ = 4.20 μM), and the introduction of substituents at R^1 improved the inhibitory activity. For example, compound **26** (2-F-3-CH_3) showed excellent inhibitory activity ($K_{i, WT}$ = 0.53 μM), equal to the commercial control bispyribac ($K_{i, WT}$ = 0.54 μM). The structure-activity relationship (SAR) can be summarized as follows: in general, compared with the substitution at

the *para*- and *ortho*- position of the substrates, substitution of groups at *meta*-position increased the enzyme inhibitory activities against wild-type *At*AHAS. For example, the inhibitory activity of compound **15** (*m*-F, $K_{i,\ WT}$ = 2.01 μM) was 6-fold higher than **16** (*p*-F, $K_{i,\ WT}$ = 11.90 μM), and 13-fold higher than **14** (*o*-F, $K_{i,\ WT}$ = 27.40 μM). Compounds with -Cl, -Me substituents followed the same trend: *m*-Cl > *p*-Cl > *o*-Cl (**18** > **19** > **17**); *m*-CH_3 > *p*-CH_3 (**13** > **12**) (Table 1).

Furthermore, the number and position of substitutions on the phenoxy group also could affect their inhibitory activity against wild-type *At*AHAS. More specifically, introducing both a *m*-methyl group and an *o*-fluoro atom at R^1, compound **26** (2-F-3-CH_3, $K_{i,\ WT}$ = 0.53 μM), produced the best inhibitory activity. From the binding models, the binding of compound **26** (Figure 5C) in wild-type *At*AHAS active channel was very similar to that of compound **11** (Figure 5B). But the introduction of *o*-F atom (compound **26**) could form a strong hydrogen bond with S654 (3.5 Å) and the introduction of the *m*-Me increased the hydrophobic interaction, which resulted in an elevation of electrostatic energy and VDW energy. Finally, compound **26** exhibited a higher binding free energy ($\Delta G_{cal,\ WT}$ = −25.60 kcal/mol) against wild-type *At*AHAS as compared with the unsubstituted compound **11** ($\Delta G_{cal,\ WT}$ = −20.81 kcal/mol) (Table 1).

The Molecular Basis of Anti-resistance Mechanism. To illuminate the relationship between the structure and resistance at molecular level, we carried out molecular simulation for representative molecules and binding free energy calculations for the synthesized derivatives. As shown in Table 1, the ranges of the calculated binding free energies (ΔG_{cal}) were from −13.98 to −25.60 kcal/mol and −12.01 to −21.74 kcal/mol for wild-type *At*AHAS

and P197L mutant respectively. More importantly, the $\Delta\Delta G$ ($\Delta G_{P197L} - \Delta G_{WT}$) indicated that the difference between the binding free energy for P197L mutant and wild-type *At*AHAS, and it can be used as a criterion to determine resistance caused by P197L mutation. The calculated $\Delta\Delta G_{cal}$ ranged from 7.26 to −0.90 kcal/mol, whereas the experimental $\Delta\Delta G_{exp}$ ranged from 7.83 to −0.77 kcal/mol. It is worth mentioning that the relative order of the calculated $\Delta\Delta G_{cal}$ of these analogues corresponded with that of actual $\Delta\Delta G_{exp}$ qualitatively ($\Delta\Delta G_{exp} = -RT \text{ Ln } K_{i,P197L}/K_{i,WT}$). A linear correlation between the calculated $\Delta\Delta G_{cal}$ and experimental $\Delta\Delta G_{exp}$ was acquired with a correlation coefficient of R^2 = 0.92 (Figure 6), which confirmed the reliability and rationality of the anti-resistance theoretical models built in this work. In addition, in order to quantitate the degree of resistance of inhibitors caused by P197L mutation, we defined the resistance factor (*RF*) as the ratio between the K_i values of the mutant to that of wild-type enzyme. This ratio was calculated for evaluating the effects of the compounds **11**–**38** on resistance ($RF = K_{i,P197L}/K_{i,WT}$). It turned out the larger the value of *RF*, the lower the drug resistance or it could be deduced that the smaller the value of $\Delta\Delta G_{cal}$, the higher drug resistance.

As shown in Table 1, the K_i values of compound **11** (unsubstituted) against P197L mutant and wild-type *At*AHAS were determined to be 52.80 μM and 4.20 μM respectively. Comparing these values indicated that the resistance factor (*RF*) value was 12.57, which was far smaller than the positive control, tribenuron-methyl with *RF* = 2650. The different substituent groups (R^1) on phenoxy ring of compound **11** could greatly affect the resistance factor (*RF*). In comparison with the parent compound **11**, the *RF* values of compounds with 3-F, 2-Cl or 3-Cl substitutions (compounds **15**, **17** or **18**) were not conducive to the reduction

283 of the resistance factor (*RF* values were increased by over 2-fold). Taking compound **15** as an
284 example, although it had a good inhibitory activity ($K_{i,\ WT}$ = 2.01 μM) against wild-type
285 *At*AHAS, its K_i value was 60.50 μM toward the P197L mutant.

286 From energy component analysis (Table S1 and Table S2), we found that the
287 electrostatic energy (ΔE_{ele}) and VDW energy (ΔE_{vdw}) of compound **15** showed a higher
288 value for wild-type *At*AHAS compared with the P197L mutant, which resulted in enthalpy
289 contribution (ΔH) to having a smaller value for wild-type *At*AHAS. Hence, the binding free
290 energy of compound **15** (ΔG_{cal} = −22.39 kcal/mol) against wild-type *At*AHAS was lower
291 than the same against P197L mutant (ΔG_{cal} = −15.30 kcal/mol) and its $\Delta\Delta G_{cal}$ value was
292 7.09 kcal/mol, which was consistent with the experimental value ($\Delta\Delta G_{exp}$ = 8.44 kcal/mol*;*
293 *RF* = 30.10). Furthermore, the compounds bearing 4-CH_3, 4-F, 3.4-benzo- and 4-Cl, 2-F-
294 substitutions (compounds **12**, **16**, **21** and **29**) had slightly lower binding affinity against the
295 P197L mutant (ΔG_{cal} = −17.54, −16.56, −21.74 and −17.73 kcal/mol respectively) than
296 against wild-type *At*AHAS (ΔG_{cal} = −18.94, −19.00, −23.38 and −19.58 kcal/mol
297 respectively). These numbers were also in good agreement with the experimental values (*RF*
298 = 1.31, 1.80, 1.77 and 1.20 respectively). These results indicated that these inhibitors had low
299 resistance level. It is fair to conclude that the compounds which had a lower binding free
300 energy against the P197L mutant than the same against wild-type *At*AHAS ($\Delta\Delta G_{cal}$ < 0
301 kcal/mol), could be considered as potential anti-resistance inhibitors. In line with this, when
302 the R^1 group on the phenoxy group changed from -H to 4-Ph, 2,3-Cl, the compounds showed
303 less resistance, for instance in compounds **22** (*RF* = 0.73) and **30** (*RF* = 0.81). However, in
304 consideration of their inhibitory activity, compound **22** appears to have a better anti-resistance

AHAS inhibitory activity simply because it had the lowest resistance factor and displayed excellent inhibitory activities against both the P197L mutant and wild-type *At*AHAS.

To explain the anti-resistance property, we investigated the binding modes using compound **22** as a representative. As depicted in Figures 5D–F, compound **22** had a conservative π-π stacking interaction with W574 and its carboxyl group could form hydrogen bonds with the residues (G120, K256, R377 and S653) of the both wild-type *At*AHAS and P197L mutant. When the amino acid residue was mutated (P197L), a steric clash occurred between L197 and the biphenyl structure of compound **22**. The flexible bridge of the molecule led to the ligand shifting deeply into the pocket, thereby increasing the VDW interactions ($\Delta\Delta E_{vdw} = -2.49$ kcal/mol). At the same time, this strengthened the hydrogen bond between the ligand and G120, but it could not compensate for the weakened hydrogen bonds between the ligand and amino acid residues R377 and K256 ($\Delta\Delta E_{ele} = 1.29$ kcal/mol). On the other hand, the mutation reduced the loss of solvation energy ($\Delta\Delta E_{pbsol} = -1.83$ kcal/mol) and increased entropy compensation ($-T\,\Delta\Delta S = 2.54$ kcal/mol). Above all, compound **22** showed better binding affinities for the P197L mutant than wild-type *At*AHAS ($\Delta\Delta G_{cal} = -0.48$ kcal/mol) (Table 1). This could also justify why compound **22** could potentially be an anti-resistance *At*AHAS inhibitor ($\Delta\Delta G_{exp} < 0$ kcal/mol, $RF < 1$).

To overcome resistance associated with AHAS mutation, we needed to consider the factors mentioned earlier (i.e. inhibitory activity and resistance factor). On the basis of above observations, compounds **21**, **22**, **26**, **33** and **38** had low *RF* values and showed excellent inhibitory activities against both wild-type *At*AHAS and P197L mutant. Notably, the inhibitory activity of compound **22** (4-Ph) was improved significantly compared to

unsubstituted compound **11** (20-fold), tribenuron-methyl (78-fold) and was equivalent to bispyribac (0.9-fold) against P197L mutant. At the same time, the *RF* value of compound **22** was also reduced about 3630-fold and 6-fold in comparison to the positive controls tribenuron-methyl and bispyribac respectively. The energy component analysis (Table 1) also showed that compound **22** had equal and low binding free energy against wild-type *At*AHAS and P197L mutant respectively, which corresponded with the experimental results.

Herbicidal Activity against Sensitive and Resistant *Descurainia sophia*. To further investigate the greenhouse *in vivo* herbicidal activity of the synthesized compounds **11**–**38**, we selected sensitive and resistant (Pro-197-Leu mutation in AHAS) *D. sophia* as representative weeds. We selected commercial AHAS herbicides tribenuron-methyl and bispyribac as controls.[46] Some of the synthesized compounds displayed promising herbicidal activity against both sensitive and resistant weeds. Furthermore, the growth of inhibited weeds could be recovered to a certain extent when we added additional branched-chain amino acids (valine, leucine and isoleucine) to the herbicidal assays (data not shown). This indicated that these compounds targeted AHAS in the tested weeds.

As shown in Table 2, most derivatives exhibited moderate to good control against sensitive *D. sophia* at the rate of 150 g ai/ha. Compounds **15**, **18**, **26**, **33, 36** and **38** clearly exhibited over 90% inhibition. Even at lower dosage of 37.5 g ai/ha, compounds **15** and **38** displayed more than 80% inhibition against the sensitive weeds, and these results were comparable to that of tribenuron-methyl and bispyribac. It can be noted that some compounds also demonstrated good herbicidal activity against resistant *D. sophia* (P197L). Compounds **21**, **22**, **26**, **31**, **33** and **36** at 150 g ai/ha showed more than 60% weed control, and compound **38** displayed almost

100% inhibition against the resistant weed, which was a stronger inhibitory effect than the tribenuron-methyl inhibition against the resistant weed. When the dosage was reduced to 37.5 g ai/ha, tribenuron-methyl showed weak herbicidal activity against the resistant *D. sophia* (<30% inhibition). In contrast, compounds **33** and **38** as well as another control, bispyribac, exhibited good inhibition (> 60%) against the resistant *D. sophia*. This was consistent with the observation from their AHAS-inhibiting activities *in vitro* against the P197L mutant (Table 1). Surprisingly, although some of the synthesized compounds had good anti-resistance properties *in vitro*, their herbicidal activities against the sensitive or resistant weeds were not satisfactory. For example, compounds **21** and **22** showed a low *RF* value and excellent inhibitory activity against the two enzymes (P197L mutant and wild-type *At*AHAS); however, their activities against the resistant and sensitive weeds could not compete with that of tribenuron-methyl and bispyribac. The main reason for such discrepancy could be that these compounds (**21** and **22**) might not possess the expected absorption, distribution, metabolism, and excretion (ADME) properties.

To summarize our findings, compounds **26**, **33**, **36** and **38** displayed good herbicidal activity against both the sensitive and resistant *D. sophia*. In particular, compounds **33** and **38** showed better or equivalent inhibition against the resistant *D. sophia* compared with tribenuron-methyl and bispyribac at three dosages (37.5, 75 and 150 g ai/ha). Therefore it can be inferred that those compounds not only ensured high herbicidal potency, but also showed better anti-resistance properties than tribenuron-methyl.

In conclusion, in this study a series of 28 hybrids of triazine-salicylic acids (phenoxy substituted) connected through an ether bridge were designed through conformational

371 flexibility and scaffold hopping. These compounds were synthesized and evaluated for their
372 *At*AHAS inhibition, anti-resistance property and herbicidal activity. Compounds **21**
373 (3,4-benzo**)**, **22** (4-Ph), **26** (2-F-3-CH_3), **33** (2-Cl-4-CH_3), **36** (3-CH_3-4-Cl) and **38**
374 (3-CH_3-4-Br) had low resistance factor (*RF* ranging from 0.73 to 6.32) and showed excellent
375 inhibitory activities against both wild-type *At*AHAS and its P197L mutant. In particular,
376 compound **22** ($K_{i,\ WT}$ = 3.69 μM, $K_{i,\ P197L}$ = 2.71 μM, *RF*=0.73) was found to be the most
377 potent anti-resistance *At*AHAS inhibitor and its resistance level was reduced about 3630-fold,
378 and 6-fold when compared with control tribenuron-methyl (*RF*=2650) and bispyribac
379 (*RF*=4.57), respectively. Computational simulations revealed that the conformational
380 flexibility of these compounds was the main reason for the low resistance causing by P197L
381 mutation. Further greenhouse *in vivo* assays showed that compounds **26**, **33**, **36** and **38**
382 displayed promising herbicidal activity against both the sensitive and resistant (P197L) *D.*
383 *sophia*. We believe that compounds **33** and **38** have the potential to overcome weed resistance
384 conferred by P197L mutant in AHAS because they maintained more than 60% inhibition
385 against both the sensitive and resistant *D. sophia* at an application rate as low as 37.5 g ai/ha.
386 On the basis of the aforementioned discussion, the designed hybrid structures can be regarded
387 as new leads for the development of anti-resistance AHAS inhibitors to overcome weed
388 resistance.
389
390 **Supporting Information**
391 Supporting Information includes the energy component analysis of compounds **11**–**38** in P197L
392 mutant and wild-type *At*AHAS (Table S1 and Table S2), inhibition curves for

compounds **22** and **38** against wild-type *At*AHAS and P197L mutant (Figure S1), the detailed synthetic procedures, physical and spectrum data of compounds **11**–**38**. This material is available free of charge via the Internet at http://pubs.acs.org.

Acknowledgment

We thank Prof. Jie Chen at Zhejiang Research Institute of Chemical Industry for her help in screening for herbicidal activity. This research was supported by the National Key R&D Program (2017YFD0200507) and the National Natural Science Foundation of China (No. 21332004).

Notes

The authors declare no competing financial interest.

REFERENCES

(1) Bar-Ilan, A.; Balan, V.; Tittmann, K.; Golbik, R.; Vyazmensky, M.; Huebner, G.; Barak, Z.; Chipman, D. M., Binding and activation of thiamin diphosphate in acetohydroxyacid synthase. *Biochemistry* **2001**, *40*, 11946-11954.

(2) Duggleby, R. G.; Pang, S. S., Acetohydroxyacid synthase. *J. Biochem. Mol. Biol.* **2000**, *33*, 1-36.

(3) Xiong, Y.; Liu, J.; Yang, G. F.; Zhan, C. G., Computational determination of fundamental pathway and activation barriers for acetohydroxyacid synthase-catalyzed condensation reactions of alpha-Keto acids. *J. Comput. Chem.* **2010**, *31*, 1592-1602.

(4) Pang, S. S.; Duggleby, R. G.; Guddat, L. W., Crystal structure of yeast acetohydroxyacid synthase: a target for herbicidal inhibitors. *J. Mol. Biol.* **2002**, *317*, 249-262.

(5) Pang, S. S.; Guddat, L. W.; Duggleby, R. G., Molecular basis of sulfonylurea herbicide inhibition of acetohydroxyacid synthase. *J. Biol. Chem.* **2003**, *278*, 7639-7644.

(6) McCourt, J. A.; Pang, S. S.; King-Scott, J.; Guddat, L. W.; Duggleby, R. G., Herbicide-binding sites revealed in the structure of plant acetohydroxyacid synthase. *Proc. Natl. Acad. Sci.* **2006**, *103*, 569-573.

(7) Garcia, M. D.; Nouwens, A.; Lonhienne, T. G.; Guddat, L. W., Comprehensive understanding of acetohydroxyacid synthase inhibition by different herbicide families. *Proc. Natl. Acad. Sci.* **2017**, *114*, 1091-1100.

(8) Duggleby, R. G.; Pang, S. S.; Yu, H.; Guddat, L. W., Systematic characterization of mutations in yeast acetohydroxyacid synthase. *Eur. J. Biochem.* **2003**, *270*, 2895-2904.

(9) Yu, Q.; Powles, S. B., Resistance to AHAS inhibitor herbicides: current understanding. *Pest Manage. Sci.* **2014**, *70*, 1340-1350.

(10) Tranel, P. J.; Wright, T. R., Resistance of weeds to ALS-inhibiting herbicides: what have we learned?. *Weed Sci.* **2002**, *50*, 700-712.

(11) Guo, Y.; Han, M.; Yan, W.; Xu, J.; Zhang, W., Generation of branched-chain amino acids resistant *Corynebacterium glutamicum* acetohydroxy acid synthase by site-directed mutagenesis. *Biotechnol. Bioprocess Eng.* **2014**, *19*, 456-467.

(12) Hamouzova, K.; Kosnarova, P.; Salava, J.; Soukup, J.; Hamouz, P., Mechanisms of resistance to acetolactate synthase- inhibiting herbicides in populations of *Apera spica*-venti from the Czech Republic. *Pest Manage. Sci.* **2014**, *70*, 541-548.

(13) Walsh, M. J.; Owen, M. J.; Powles, S. B., Frequency and distribution of herbicide resistance in *Raphanus raphanistrum* populations randomly collected across the western Australian wheatbelt. *Weed Res.* **2007**, *47*, 542-550.

(14) Heap, I. The International Survey of Herbicide-Resistant Weeds. www.weedscience.org (Accessed: 10 July 2017).

(15) Beckie, H. J.; Warwick, S. I.; Sauder, C. A.; Lozinski, C.; Shirriff, S., Occurrence and molecular characterization of acetolactate synthase (ALS) inhibitor-resistant kochia (*Kochia scoparia*) in western Canada. *Weed Technol.* **2011**, *25*, 170-175.

(16) Legere, A.; Stevenson, F. C.; Beckie, H. J.; Warwick, S. I.; Johnson, E. N.; Hrynewich, B.; Lozinski, C., Growth characterization of kochia (*Kochia scoparia*) with substitutions at Pro(197) or Trp(574) conferring resistance to acetolactate synthase-inhibiting herbicides. *Weed Sci.* **2013**, *61*, 267-276.

(17) Intanon, S.; Perez-Jones, A.; Hulting, A. G.; Mallory-Smith, C. A., Multiple Pro(197) ALS substitutions endow resistance to ALS inhibitors within and among mayweed chamomile populations. *Weed Sci.* **2011**, *59*, 431-437.

(18) Kolkman, J. M.; Slabaugh, M. B.; Bruniard, J. M.; Berry, S.; Bushman, B. S.; Olungu, C.; Maes, N.; Abratti, G.; Zambelli, A.; Miller, J. F.; Leon, A.; Knapp, S. J., Acetohydroxyacid synthase mutations conferring resistance to imidazolinone or sulfonylurea herbicides in sunflower. *Theor. Appl. Genet.* **2004**, *109*, 1147-1159.

(19) Lang, Z. F.; Shen, J. J.; Cai, S.; Zhang, J.; He, J.; Li, S. P., Expression, characterization, and site-directed mutation of a multiple herbicide-resistant acetohydroxyacid synthase (rAHAS) from *Pseudomonas* sp. Lm10. *Curr. Microbiol.* **2011**, *63*, 145-150.

(20) Guttieri, M.J., Eberlein, C.V., Mallory-Smith, C.A., Thill, D.C. and Hoffman, D.L., DNA sequence variation in domain A of the acetolactate synthase genes of herbicide-resistant and -susceptible weed biotypes. *Weed Sci.* **1992**, *40*, 670-677.

(21) Choe, M.; Choe, W.; Lee, I.; Wu, M.; Liu, S., Computational analysis of mutated AHAS in response to sulfonylurea herbicides. *Weed Res.* **2015**, *55*, 359-369.

(22) Kawai, K.; Kaku, K.; Izawa, N.; Shimizu, M.; Kobayashi, H.; Shimizu, T., Herbicide sensitivities of mutated enzymes expressed from artificially generated genes of acetolactate synthase. *J. Pestic. Sci.* **2008**, *33*, 128-137.

(23) Sibony, M.; Michel, A.; Haas, H. U.; Rubin, B.; Hurle, K., Sulfometuron-resistant *Amaranthus retroflexus*: cross-resistance and molecular basis for resistance to acetolactate synthase-inhibiting herbicides. *Weed Res.* **2001**, *41*, 509-522.

(24) Uchino, A.; Ogata, S.; Kohara, H.; Yoshida, S.; Yoshioka, T.; Watanabe, H., Molecular basis of diverse responses to acetolactate synthase-inhibiting herbicides in sulfonylurea-resistant biotypes of *Schoenoplectus juncoides*. *Weed Biol. Manage.* **2007**, *7*, 89-96.

(25) Cui, H. L.; Li, X.; Wang, G.; Wang, J.; Wei, S.; Cao, H., Acetolactate synthase proline (197) mutations confer tribenuron-methyl resistance in *Capsella bursa-pastoris* populations from China. *Pestic. Biochem. Physiol.* **2012**, *102*, 229-232.

(26) Delye, C.; Causse, R.; Michel, S., Genetic basis, evolutionary origin and spread of resistance to herbicides inhibiting acetolactate synthase in common groundsel (*Senecio vulgaris*). *Pest Manage. Sci.* **2016**, *72*, 89-102.

(27) Marshall, R.; Hull, R.; Moss, S. R., Target site resistance to ALS inhibiting herbicides in

Papaver rhoeas and *Stellaria media* biotypes from the UK. *Weed Res.* **2010**, *50*, 621-630.

(28) Ji, F. Q.; Niu, C. W.; Chen, C. N.; Chen, Q.; Yang, G. F.; Xi, Z.; Zhan, C. G., Computational design and discovery of conformationally flexible inhibitors of acetohydroxyacid synthase to overcome drug resistance associated with the W586L mutation. *ChemMedChem* **2008**, *3*, 1203-1206.

(29) Yu, Z.; Wen, X.; Xi, Z., Insight into herbicide resistance of W574L mutant *Arabidopsis thaliana* acetohydroxyacid synthase: molecular dynamics simulations and binding free energy calculations. *Sci. China Chem.* **2010**, *53*, 91-102.

(30) He, Y.; Niu, C.; Li, H.; Wen, X.; Xi, Z., Experimental and computational correlation and prediction on herbicide resistance for acetohydroxyacid synthase mutants to bispyribac. *Sci. China Chem.* **2013**, *56*, 286-295.

(31) He, Y.; Niu, C.; Wen, X.; Xi, Z., Molecular drug resistance prediction for acetohydroxyacid synthase mutants against chlorsulfuron using MB-QSAR. *Chin. J. Chem.* **2013**, *31*, 1171-1180.

(32) Qu, R. Y.; Liu, Y. C.; Wu, Q. Y.; Chen, Q.; Yang, G. F., An efficient method for syntheses of functionalized 6-bulkysubstituted salicylates under microwave irradiation. *Tetrahedron* **2015**, *71*, 8123-8130.

(33) Liu, Y. C.; Qu, R. Y.; Chen, Q.; Yang, J. F.; Niu, C. W.; Zhen, X.; Yang, G. F., Triazolopyrimidines as a new herbicidal lead for combating weed resistance associated with acetohydroxyacid synthase mutation. *J. Agric. Food. Chem.* **2016**, *64*, 4845-4857.

(34) Qu, R. Y.; Yang, J. F.; Liu, Y. C.; Chen, Q.; Hao, G. F.; Niu, C. W.; Xi, Z.; Yang, G. F., Computational design of novel inhibitors to overcome weed resistance associated with

503 acetohydroxyacid synthase (AHAS) P197L mutant. *Pest Manag. Sci.* **2017**, *73*, 1373-1381.

504 (35) Xiong, L.; Zhu, X. L.; Gao, H. W.; Fu, Y.; Hu, S. Q.; Jiang, L. N.; Yang, W. C.; Yang,

505 G. F., Discovery of potent succinate-ubiquinone oxidoreductase inhibitors via

506 pharmacophore-linked fragment virtual screening approach. *J. Agric. Food. Chem.* **2016**, *64*,

507 4830-4837.

508 (36) He, Y. Z.; Li, Y. X.; Zhu, X. L.; Xi, Z.; Niu, C.; Wan, J.; Zhang, L.; Yang, G. F.,

509 Rational design based on bioactive conformation analysis of pyrimidinylbenzoates as

510 acetohydroxyacid synthase inhibitors by integrating molecular docking, CoMFA, CoMSIA,

511 and DFT calculations. *J. Chem. Inf. Model.* **2007**, *47*, 2335-2344.

512 (37) Ruiz-Santaella, J. P.; Heredia, A.; De Prado, R., Basis of selectivity of cyhalofop-butyl

513 in *Oryza sativa* L. *Planta* **2006,** *223*, 191-199.

514 (38) Oliveira Neto, A. M.; Constantin, J.; Oliveira Jr, R. S.; Barroso, A. L. L.; Braz, G. B. P.;

515 Guerra, N.; Gheno, E. A., Selectivity of fomesafen to cotton. *Planta Daninha* **2015**, *33*,

516 759-770.

517 (39) Sada, Y.; Ikeda, H.; Kizawa, S., Resistance levels of sulfonylurea-resistant

518 *Schoenoplectus juncoides* (Roxb.) Palla with various Pro197 mutations in acetolactate

519 synthase to imazosulfuron, bensulfuron-methyl, metsulfuron-methyl and

520 imazaquin-ammonium. *Weed Biol. Manage.* **2013**, *13*, 53-61.

521 (40) Boigegrain, R. A.; Liautard, J. P.; Kohler, S., Targeting of the virulence factor

522 acetohydroxyacid synthase by sulfonylureas results in inhibition of intramacrophagic

523 multiplication of *Brucella suis*. *Antimicrob. Agents Chemother.* **2005**, *49*, 3922-3925.

524 (41) The Cambridge Crystallographic Data Centre (CCDC). https://www.ccdc.cam.ac.uk/

(Accessed: 06 June 2017).

(42) Singh, B. K.; Stidham, M. A.; Shaner, D. L., Assay of acetohydroxyacid synthase. *Anal. biochem.* **1988**, *171*, 173-179.

(43) Li, Y. X.; Luo, Y. P.; Xi, Z.; Niu, C. W.; He, Y. Z.; Yang, G. F., Design and syntheses of novel phthalazin-1(2H)-one derivatives as acetohydroxyacid synthase inhibitors. *J. Agric. Food. Chem.* **2006**, *54*, 9135-9139.

(44) Chang, A. K.; Duggleby, R. G., Herbicide-resistant forms of *Arabidopsis thaliana* acetohydroxyacid synthase: characterization of the catalytic properties and sensitivity to inhibitors of four defined mutants. *Biochem. J.* **1998**, *333* , 765-777.

(45) Sitkoff, D.; Sharp, K. A.; Honig, B., Accurate calculation of hydration free energies using macroscopic solvent models. *J. Phys. Chem.* **1994**, *98*, 1978-1988.

(46) Cui, H. L.; Zhang, C. X.; Wei, S. H.; Zhang, H. J.; Li, X. J.; Zhang, Y. Q.; Wang, G. Q., Acetolactate synthase gene proline (197) mutations confer tribenuron-methyl resistance in flixweed (*Descurainia sophia*) populations from China. *Weed Sci.* **2011**, *59*, 376-379.

FIGURE CAPTIONS:

Figure 1. Chemical structures of commercial AHAS inhibitors.

Figure 2. Design strategy of the novel anti-resistance AHAS compounds.

Figure 3. Synthetic route of the title compounds **11**–**38**. Reagents and Conditions: (i) *n*-BuLi, TMEDA, DIPA, DMF, -78 °C; (ii) K_2CO_3, DMF, 100 °C; (iii) KOH, 30% H_2O_2, CH_3OH, 60 °C; (iv) BBr_3, CH_2Cl_2, -78 °C; (v) $KHCO_3$, DMF, 100 °C; (vi) K_2CO_3, DMF, 60 °C; (vii) H_2, Pd/C(10%), CH_3OH, AcOH, RT.

Figure 4. X-ray crystal structures for compound **22**.

Figure 5. (A) The binding mode of compound **21** in P197L mutant interaction; (B and C) Binding modes for compounds **11** and **26** interactions with wild-type *At*AHAS; (D and E) Binding modes of compound **22** interactions with wild-type *At*AHAS and P197L mutant; (F) Binding mode for compound **22** interactions with wild-type *At*AHAS (blue), and the P197L mutant (green) are overlaid. [Simulated binding modes of the interaction between representative compounds (**11**, **21**, **22** and **26**) and wild-type *At*AHAS or P197L mutant. The black dashed lines represent hydrogen bonds between ligands and key residues].

Figure 6. The correlation between the difference of calculated and experimental binding free energy ($\Delta\Delta G$).

Table 1. Inhibitory Activities and the Binding Free Energy of Compounds **11**–**38** against Wild-Type *At*AHAS and P197L Mutant.

Compd.	R^1	K_i (μM)		ΔG_{cal} (kcal/mol)		*RF*[a]	$\Delta\Delta G$ (kcal/mol)	
		Wild-Type *At*AHAS	P197L Mutant	Wild-Type *At*AHAS	P197L Mutant		$\Delta\Delta G_{cal}$	$\Delta\Delta G_{exp}$[b]
11	H	4.20 ± 0.37	52.80 ± 7.50	−20.81	−15.72	12.57	5.09	6.27
12	4-CH_3	17.80 ± 1.60	23.40 ± 1.70	−18.94	−17.54	1.31	1.40	0.68
13	3-CH_3	6.45 ± 1.20	20.10 ± 1.90	−20.15	−17.79	3.12	2.36	2.82
14	2-F	27.40 ± 9.90	108.00 ± 11.00	−17.34	−14.72	3.94	2.62	3.40
15	3-F	2.01 ± 0.46	60.50 ± 9.40	−22.39	−15.30	30.10	7.09	8.44
16	4-F	11.90 ± 1.10	21.4 ± 2.50	−19.00	−16.56	1.80	2.44	1.45
17	2-Cl	8.27 ± 9.60	212.00 ± 23.00	−19.17	−12.63	25.63	6.54	8.04
18	3- Cl	1.84 ± 0.36	43.40 ± 6.70	−23.21	−15.94	23.59	7.26	7.83
19	4- Cl	4.51 ± 0.37	56.00 ± 7.20	−20.27	−15.76	12.42	4.51	6.24
20	2-Br	25.70 ± 6.40	65.70 ±7.50	−19.05	−16.16	2.55	2.88	2.33
21	3.4-benzo	1.79 ± 0.18	3.17 ± 0.15	−23.38	−21.74	1.77	1.64	1.42
22	4-Ph	3.69 ± 0.89	2.71 ± 0.12	−20.69	−21.17	0.73	−0.48	−0.77
23	2,3-diF	15.8 ± 1.90	228.00 ± 24.00	−18.90	−12.01	14.43	6.89	6.62
24	2,4-diF	14.70 ± 3.60	84.30 ± 7.00	−19.84	−14.86	5.73	4.98	4.33
25	2,5-diF	5.72 ± 1.36	26.30 ± 3.90	−20.95	−17.48	4.59	3.46	3.78
26	3-CH_3-2-F	0.53 ± 0.03	3.35 ± 0.42	−25.60	−21.72	6.32	3.88	4.57
27	4-CH_3-2-F	6.07 ± 0.79	20.20 ± 1.80	−21.12	−17.19	3.33	3.93	2.98
28	5-CH_3-2-F	5.37 ± 0.65	61.2 ± 7.20	−21.34	−16.53	11.40	4.81	6.03
29	2-F-4-Cl	15.70 ± 2.30	18.90 ± 2.70	−19.58	−17.73	1.20	1.85	0.46
30	2,3-diCl	92.90 ± 9.90	75.70 ± 7.80	−13.98	−14.88	0.81	−0.90	−0.51
31	2,4-diCl	2.12 ± 0.35	7.58 ± 1.02	−22.55	−20.11	3.58	2.44	3.16
32	2,5-diCl	14.40 ± 2.50	55.30 ± 6.50	−18.55	−16.37	3.84	2.19	3.34
33	2-Cl-4-CH_3	1.59 ± 0.45	3.70 ± 0.51	−23.18	−21.62	2.33	1.56	2.09
34	2-Br-4-F	4.58 ± 1.22	47.0 ± 3.80	−21.60	−16.37	10.26	5.24	5.77
35	2-CH_3-4-Cl	3.25 ± 0.56	9.16 ± 1.71	−21.75	−19.54	2.82	2.22	2.57
36	3-CH_3-4-Cl	1.34 ± 0.28	6.42 ± 0.80	−23.61	−20.44	4.79	3.17	3.88
37	3-Br-4-F	6.94 ± 0.68	145.00 ± 15.00	−19.69	−13.21	20.89	6.48	7.53
38	3-CH_3-4-Br	1.41 ± 0.28	3.34 ± 0.40	−23.27	−21.11	2.37	2.16	2.14
Tribenuron-methyl		0.08 ± 0.01	212.00 ± 47.00	−29.73	−12.77	2650	16.96	24.33
Bispyribac		0.54 ± 0.06	2.47 ± 0.41	−25.42	−22.14	4.57	3.28	3.76

[a] $RF = K_{i,\ P197L}/\ K_{i,\ WT}$; [b] $\Delta\Delta G_{exp} = -RT\ \mathrm{Ln}(K_{i,\ P197L}/\ K_{i,\ WT})$.

Table 2. Herbicidal Activity of Compounds **11**–**38** against Sensitive and Resistant *D.sophia*[a].

Compd.	Dose (g ai/ha)	Sensitive *D.sophia*	Resistant *D.sophia*[b]	Compd.	Dose (g ai/ha)	Sensitive *D.sophia*	Resistant *D.sophia*[b]
11	150	++++[c]	++	**27**	150	++++	++
12	150	+++	++	**28**	150	+++	+
13	150	++++	++	**29**	150	++	+
14	150	++++	−	**30**	150	+	−
15	150	+++++	++	**31**	150	++++	+++
	75	++++	−		75	+++	+
	37.5	++++	−		37.5	+	−
16	150	++++	++	**32**	150	+++	+
17	150	+++++	−	**33**	150	+++++	++++
18	150	+++++	++		75	+++++	+++
	75	++++	+		37.5	+++	+++
	37.5	+++	−	**34**	150	++++	+
19	150	++++	+	**35**	150	+++	++
20	150	+++	+	**36**	150	+++++	+++
21	150	++++	+++		75	+++++	+
	75	++	++		37.5	+++	−
	37.5	+	−	**37**	150	+++	−
22	150	+++	+++	**38**	150	+++++	+++++
	75	++	++		75	+++++	++++
	37.5	−	−		37.5	++++	+++
23	150	+++	−	**Tribenuron-**	150	+++++	+++
24	150	++++	−	**methyl**	75	+++++	++
25	150	++++	++		37.5	+++++	+
26	150	+++++	++++	**Bispyribac**	150	+++++	+++++
	75	++++	+++		75	++++	+++
	37.5	++	++		37.5	++++	+++

[a]Abbreviations: *D.sophia*: *Descurainia sophia*. [b]The mutation site of resistant *D.sophia*: Pro-197-Leu in AHAS. [c]Rating scale of herbicidal activity (percentage of inhibition): +++++, ≥90%; ++++, 80−89%; +++, 60−79%; ++, 30−59%; +, 10−29%; −, <10%.

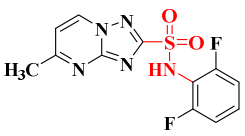

Flumetsulam
triazolopyrimidine-sulfonamides (TP)

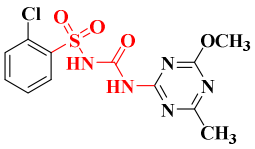

Chlorsulfuron
sulfonylureas (SU)

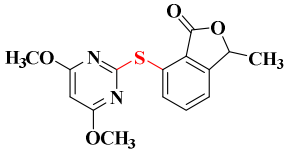

Pyriftalid
pyrimidinylthiobenzoates (PTB)

Propoxycarbazone
sulfanilamide-carbonyl-thiazolidinones (SCT)

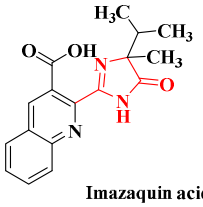

Imazaquin acid
imidazolinones (IMI)

Figure 1.

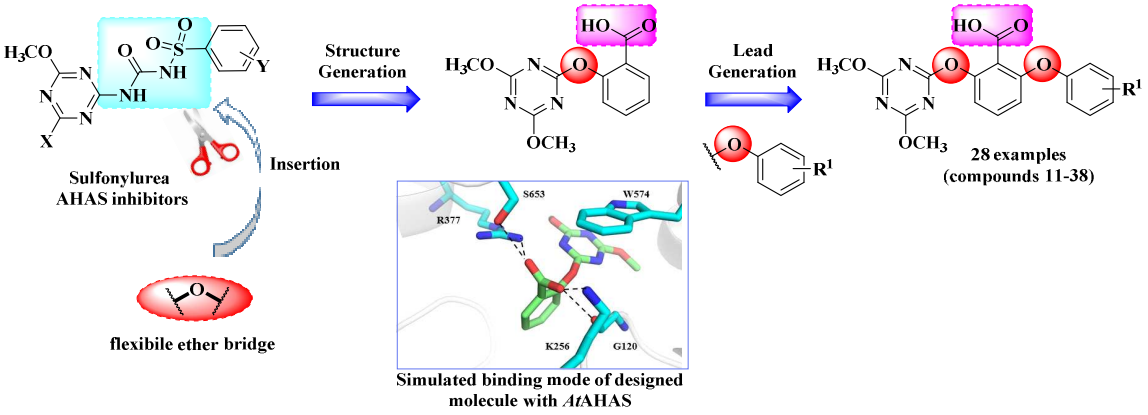
Structure Generation
Lead Generation
Sulfonylurea AHAS inhibitors
Insertion
flexibile ether bridge
28 examples (compounds 11-38)
S653
W574
R377
K256
G120
Simulated binding mode of designed molecule with AtAHAS

Figure 2.

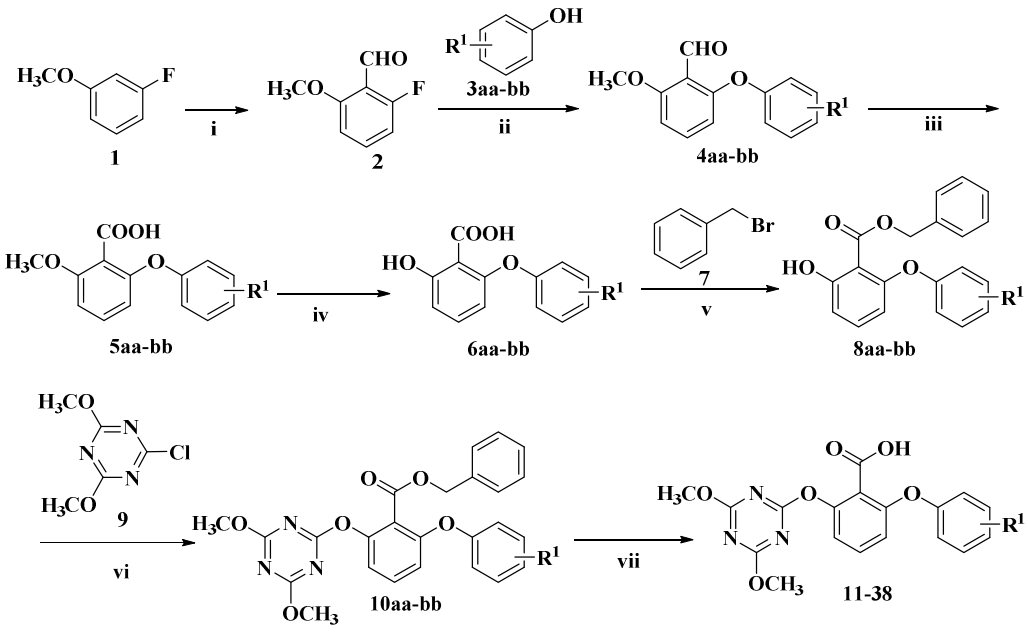
H3CO
F
1
i
CHO
2
R1
OH
3aa-bb
ii
4aa-bb
iii
COOH
5aa-bb
iv
6aa-bb
Br
7
v
8aa-bb
Cl
9
vi
10aa-bb
vii
OH
OCH3
11-38

Figure 3.

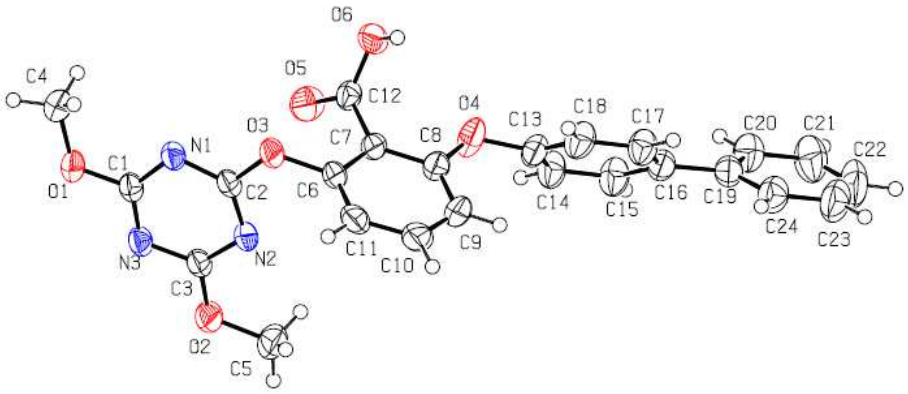
O6
O5
C12
C4
O4
C13
C18
C17
C20
C21
C22
O3
C7
C8
N1
C1
C2
C6
O1
C14
C15
C16
C19
C24
C23
C11
C10
C9
N3
N2
C3
O2
C5

Figure 4.

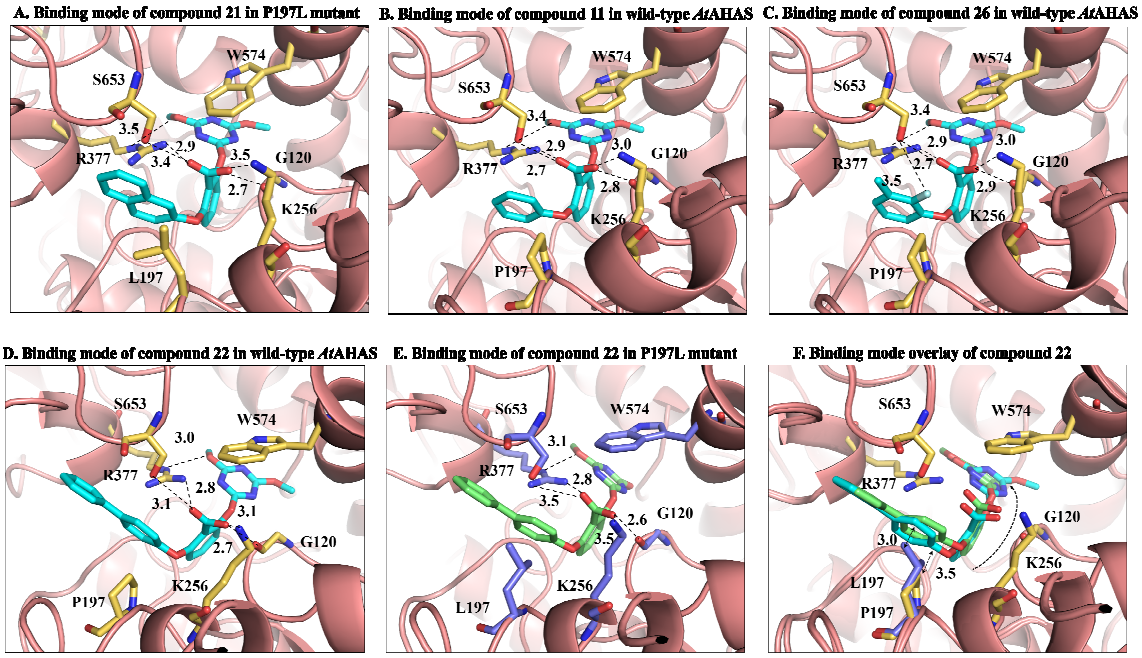
A. Binding mode of compound 21 in P197L mutant
W574
S653
3.5
2.9
R377
3.4
3.5
G120
2.7
K256
L197
B. Binding mode of compound 11 in wild-type AtAHAS
W574
S653
3.4
2.9
3.0
R377
2.7
G120
2.8
K256
P197
C. Binding mode of compound 26 in wild-type AtAHAS
W574
S653
3.4
2.9
3.0
R377
2.7
G120
3.5
2.9
K256
P197
D. Binding mode of compound 22 in wild-type AtAHAS
S653
W574
3.0
R377
2.8
3.1
3.1
2.7
G120
K256
P197
E. Binding mode of compound 22 in P197L mutant
S653
W574
3.1
R377
2.8
3.5
2.6
G120
3.5
K256
L197
F. Binding mode overlay of compound 22
S653
W574
R377
G120
3.0
3.5
K256
L197
P197

Figure 5.

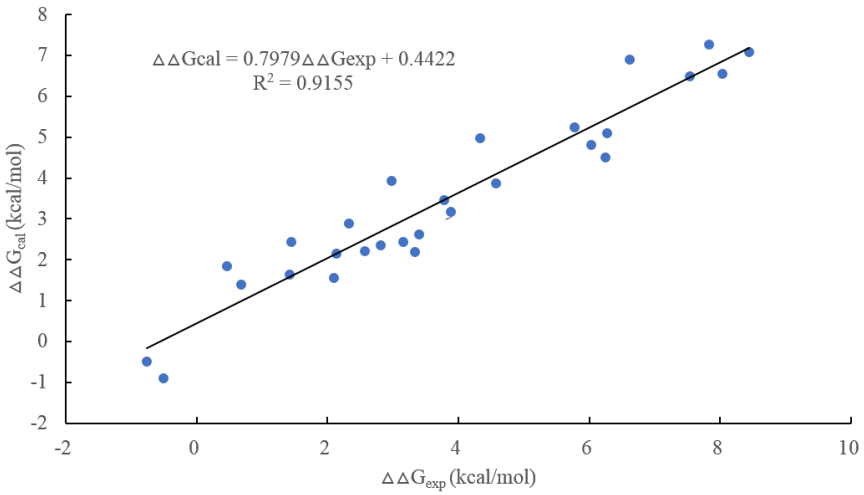
△△Gcal = 0.7979△△Gexp + 0.4422
R2 = 0.9155
△△Gcal (kcal/mol)
△△Gexp (kcal/mol)
8
7
6
5
4
3
2
1
0
-1
-2
-2
0
2
4
6
8
10

Figure 6.

Table of Contents Graphic